Surface dynamics and friction of K/Cu(001) characterized by helium-3 spin-echo and density functional theory

H. Hedgeland,[*] P. R. Kole, H. R. Davies, A. P. Jardine, G. Alexandrowicz,[†] W. Allison, and J. Ellis
Cavendish Laboratory, University of Cambridge, JJ Thomson Avenue, Cambridge CB3 0HE, United Kingdom

G. Fratesi and G. P. Brivio
ETSF, CNISM, and Dipartimento di Scienza dei Materiali, Università di Milano–Bicocca, Via Cozzi 53, 20125 Milano, Italy

Helium-3 spin-echo measurements of K/Cu(001) are presented, the diffusional surface dynamics of the system at low coverages and on picosecond time scales. Langevin molecular-dynamics simulations are used, together with a potential-energy surface derived from density functional theory calculations, to provide further understanding of the experimental data. An anisotropic potential with a corrugation of 35–64 meV and a friction parameter of $1/4.5$ ps^{-1} are found to give a good fit to the data for the lower coverages with the adsorbate interactions modeled with a dipole-dipole repulsion. Additionally, at the highest coverage, $\theta = 0.084$, a component of motion is observed perpendicular to the surface, analogous to that recently found for Na/Cu(001).

PACS number(s): 68.35.Fx, 68.35.Ja, 68.43.−h

I. INTRODUCTION

Alkali metals adsorbed on metal surfaces are not only of fundamental scientific interest but are also of technological relevance due to the ability of the adsorbate to modify the electronic structure of the surface and its resultant chemical properties.[1] Numerous experimental studies have built a picture of alkali-metal surface adsorption.[2] In general terms, alkalis show a significant amount of electronic polarization to the surface at low coverages with the polarization decreasing as the coverage increases and interadsorbate interactions become more significant.

A detailed characterization of alkali systems further provides an important benchmark for *ab initio* theoretical approaches. In particular, density functional theory (DFT) has been widely used to understand basic aspects of alkali-metal adsorption.[3–7] Therefore, it is of special interest to probe the accuracy of such a method when applied, for example, to the evaluation of diffusion energy barriers for adsorbed alkali atoms, since these are typically small (tens of meV) and close the present limit of numerical accuracy. At the same time, detailed information on the complex dynamics of these systems can be accessed by high-resolution helium atom scattering experiments, as shown by recent investigations of Na/Cu(001) (Ref. 8) and Cs/Cu(001).[9]

Previous studies of K/Cu(001) have focused mainly on adsorbate structure, vibrations, and adsorption kinetics,[10–18] rather than adsorbate diffusion. Low-energy electron-diffraction (LEED) investigations of K/Cu(001) have mapped a series of growth phases seen during adsorption.[13,16] At low temperatures and low coverages, the strong repulsive interaction between the adsorbate atoms leads to a uniform distribution across the surface, maximizing the interadsorbate spacing and forming hexagonal or quasihexagonal structures. During this initial stage of adsorption, diffraction rings have been reported.[11,12] As the coverage is increased, the adsorbate layer depolarizes and forms a continuous metallic film. The hexagonal structure becomes incommensurate to the substrate and the coverage

(defined as number of adsorbate atoms per substrate atom) is finally seen to saturate at $\theta = 0.37$ with a spacing of 4.57 Å.[10,11] Structural studies using surface x-ray diffraction and LEED identify the adsorption site for the low-coverage regime as the fourfold hollow site with the site shifting partially to a lower-symmetry site as the coverage is increased.[14–16]

Time of flight (TOF) has previously been used to measure the parallel vibrational (*t*-mode) frequencies of low coverages of a number of alkali metals on Cu(001), including potassium.[17] The potassium *t* mode was seen to have a frequency of 2.8 meV with a width of 0.7 meV when convolved with the experimental linewidth. An estimate of the friction, η, on the adatom motion derived from the elastic continuum theory,[19] gives a relaxation time, $\tau = 1/\eta$, for adsorbate-substrate energy exchange of 38 ps.[17]

In the present work we describe helium-3 spin-echo data on the surface dynamics of low coverages ($\theta < 0.085$) of K/Cu(001). DFT calculations are used to produce an adsorbate-substrate potential-energy surface (PES) for the system and model the adsorbate interations, which are compared with experimental data. The degree of agreement shown allows us to comment upon the validity of modeling adsorbate interactions with a simple dipole model. Furthermore, a value for the adsorbate-substrate kinetic friction is obtained and compared with the one previously derived from elastic continuum theory.[17] We also observe vertical motion of the potassium at high coverage. A similar phenomenon was observed recently in Na/Cu(001) (Ref. 8) and has been ascribed to fluctuations in the surface charge density rather than motion of the Na-ion cores.[20,21] The new results are important for developing our understanding of the adsorption and diffusion of alkali metals, highlighting the sensitivity of helium scattering to the electronic contribution to the measured dynamics.

The paper is organized as follows. Section II overviews the experimental technique, whose results are presented in Sec. III. The description of DFT calculations follows in Sec. IV. *Ab initio* results are then used for molecular-dynamics (MD) simulations, which are presented in Sec. V in compari-

son with experimental findings. Finally, Sec. VI is devoted to the conclusions.

II. EXPERIMENTAL PROCEDURE

A detailed description of our experimental technique, and more generally the spin-echo method, has been given previously (in particular, we refer to Refs. 22–24) so we shall only summarize the process briefly here. A beam of spin-polarized helium-3 atoms is split into two spin components by a magnetic field. The wave packets propagate at different velocities in the field, so reaching the sample, and scattering from the surface, with a time delay, that is, known as the spin-echo time, t_{se}. Recombining the two wave packets gives a measured polarization of $I(\Delta \mathbf{K}, t_{se})/I(\Delta \mathbf{K}, 0)$ at the detector, where $I(\Delta \mathbf{K}, t_{se})$ is known as the intermediate scattering function (ISF) and $\Delta \mathbf{K}$ is the momentum transfer parallel to the surface. The intermediate scattering function is a correlation measurement on a specific length scale and is the temporal Fourier transform of the dynamic structure factor $S(\Delta \mathbf{K}, \omega)$ measured in an ideal TOF experiment as well as the spatial transform of the well-established Van Hove pair-correlation function, $G(\mathbf{R}, t)$, describing the surface dynamics.[25] By examining the variation in the ISF across a range of experimental conditions (varying temperature, coverage, and momentum transfer), we can build up a detailed, microscopic picture of the motion on the surface.

The experimental data presented here was measured using the Cambridge ^{3}HeSE spectrometer.[26] A single-crystal Cu(001) sample was mounted on the six-axis manipulator in the UHV sample chamber with a base pressure of 1×10^{-10} mbar and was cleaned by repeated cycles of argon-ion sputtering (800 eV, 10 μA, 10 min at 300 K) and annealing (800 K, 30 s). Prior to the experiments, the crystal was aligned using the helium diffraction peaks from a CO overlayer. The surface quality was monitored through the sample's reflectivity to the helium beam and the shape and intensity of the helium scattering specular peak. Throughout the experiments a helium beam energy of 10 meV was used.

Potassium overlayers were prepared at a surface temperature of 200 K using a potassium dispenser (Saes Getters), where there was a maximum pressure rise during dispensing of 4×10^{-10} mbar. The helium beam specular intensity was monitored during deposition, first decreasing, then recovering to a maximum, a behavior similar to that observed widely in previous helium scattering measurements such as Ref. 18. The maximum coverage, $\theta = 0.37$, corresponds to the maximum in the specularly scattered intensity, which may be identified with the ordered structure seen by Aruga *et al.*[11] in their LEED study. The uptake curves can be used to determine the submonolayer coverages studied here, by assuming constant dose rate and sticking coefficient, as previously seen to be valid for low coverages of other alkali metals.[17,18] We note that our method shows reasonable agreement with estimates of the surface coverage from the positions of the de Gennes[27] narrowing features[28] seen in the experimental data, further validating the assumptions.

III. EXPERIMENTAL RESULTS AND OBSERVATIONS

Spin-echo measurements were made for potassium coverages between $\theta = 0.018-0.084$ at 155 K for a range of sur-

face parallel momentum transfers up to 1 Å^{-1} along the [100] azimuth, and at the lowest coverage in the [110] direction. The scattered helium intensity was found to decrease rapidly as both the momentum transfer and the coverage increased, limiting the range of measurements that could be obtained. At coverages greater than $\theta = 0.084$, multiphonon processes dominate the scattering leaving insufficient diffusion related signal for useful analysis. However, in addition to the momentum-transfer dependency, a selected subset of measurements was made over a temperature range of 155–200 K at a coverage of $\theta = 0.056$ and momentum transfer of 0.5 Å^{-1}. For all experiments, both the real and imaginary components of the polarization, $I(\Delta \mathbf{K}, t_{se})/I(\Delta \mathbf{K}, 0)$, were determined as a function of spin-echo time, corresponding to cosine and sine transforms of $S(\Delta \mathbf{K}, \omega)$, respectively (details of the measurement process are given in Ref. 23).

Using the spin-echo technique, we observe the complete ISF, which contains the signatures of several dynamical processes. In the main panels, the results are plotted using a logarithmic time axis to illustrate the different time scales. An example is given in Fig. 1, where the upper panel shows a measurement at low coverage. Two main processes can be seen in the real part of the polarization [upper curve of Fig. 1(a)]: an oscillatory component is present at small spin-echo times; a smooth exponential decay, shown by the bold line (blue online), emerges at longer spin-echo times. The oscillatory component is shown in the inset, for clarity, where the time axis is now linear. A corresponding feature is also evident in the imaginary part of the polarization (dotted curve, red online). The oscillating component corresponds to single-phonon scattering from the substrate. The smooth decay seen in the real part at large spin-echo times corresponds to loss of correlation due to hopping of the mobile potassium atoms. A comparison with data at higher coverage, see Fig. 1(b) shows that, while the signature of diffusion is still evident in the real part of the polarization at long spin-echo times, the well-defined frequency of the surface phonon, seen at low coverage, is largely absent. In its place there is a rapid polarization decay with no characteristic frequency (shown for clarity in the inset). Single-phonon scattering from the substrate has been replaced by multiphonon scattering from the adsorbate layer. By careful modeling of the various components we are able to separate them and extract each one with a high accuracy. We will now focus on the slow decay which corresponds to the quasielastic broadening of the helium beam energy profile.

Examining the decay at longer spin-echo time, we find the data is well described by a single exponential, $Ae^{(-\alpha t)}$, (bold line in Fig. 1), which corresponds to a Lorentzian line shape in the energy domain. The dephasing rate of the decay, α, is related to the full width half maximum of the quasielastic energy broadening such that $\Delta E = 2\hbar \alpha$. We find that a single exponential decay is a good fit to the large spin-echo times for all the low-coverage data ($\theta < 0.05$), suggesting a simple diffusion process,[22] and we use that data later for comparison with molecular-dynamics calculations.

The situation is more complex at the highest coverage, $\theta = 0.084$, specifically for small momentum transfers. Here, we see a significant deviation from the single exponential form. The effect is illustrated in Fig. 2, where data obtained
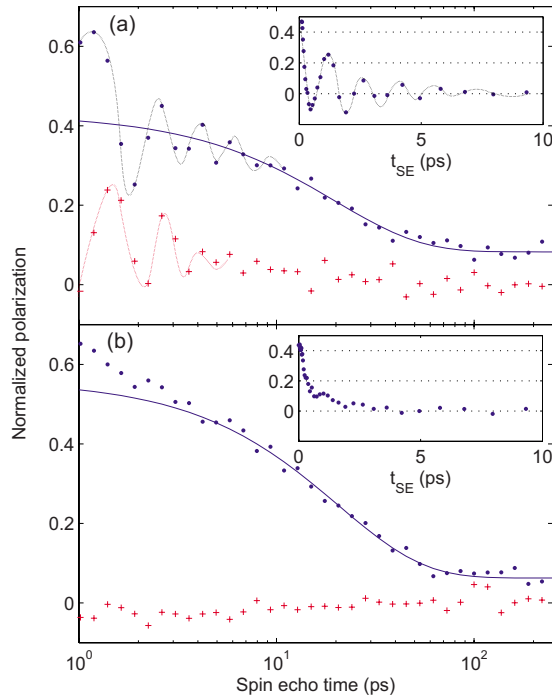
FIG. 1. (Color online) Measurements of the normalized polarization $I(\Delta\mathbf{K}, t_{se})/I(\Delta\mathbf{K}, 0)$ as a function of spin-echo time for K/Cu(001) at a momentum transfer of 0.5 Å^{-1}. The real part of the polarization is shown by (blue) points and the imaginary part by (red) crosses and the data are plotted with a logarithmic time axis to emphasize the time separation of the fast and slow components of the motion. Insets plot the real part only with a linear time axis and the slow decay subtracted. (a) (Upper plot) shows a typical example of data at low coverage: $\theta = 0.018$. (b) (Lower plot) shows data at higher coverage of $\theta = 0.045$. In both plots, the bold line is an exponential decay, fitted to the data at long spin-echo time ($t_{se} > 10$ ps), which correspond to quasielastic scattering. The fine dotted line in panel (a) indicates the single phonon contributions at low coverages and small spin-echo times and is drawn as a guide to the eye.

FIG. 2. (Color online) The real part of the measured polarization plotted against a logarithmic time axis for a potassium coverage of $\theta = 0.084$. (a) shows the behavior at small momentum transfer at $\Delta\mathbf{K} = 0.025$ Å^{-1}. (b) gives data for larger momentum transfer at $\Delta\mathbf{K} = 0.613$ Å^{-1}. A single exponential (solid curve) gives a good description of the data at high-momentum transfer (b) while the data at small momentum transfer (a) requires two exponentials to provide an adequate description (solid line). The behavior is a signature of vertical motion (see text).

at the highest coverage is shown for both low- and high-momentum transfer. The lower panel, Fig. 2(b), shows the simpler case seen at high-momentum transfer. Here, as before, a single exponential curve (solid line) provides an accurate description of the data. The behavior at small momentum transfer, shown in Fig. 2(a) requires two exponential functions, shown by the solid line, to describe the measurements accurately, implying processes with two different time scales are occurring on the surface. The phenomenon is illustrated further in Fig. 3, where the dephasing rates extracted from the data are shown for momentum transfers up to 0.2 Å. The two components have a strikingly different behavior. The slow component, shown in Fig. 3 by open circles, displays a strong dependence on momentum transfer with $\alpha \to 0$ at low-momentum transfer. Such behavior is expected of motion parallel to the surface[28] and it agrees well with calculations for pure, planar motion (solid line), described later. In contrast, the fast component is independent of momentum transfer, within the noise on the data, and has a dephasing rate of approximately 0.2 ps^{-1}. (It may be noted that the uncertainty at small times is much more significant
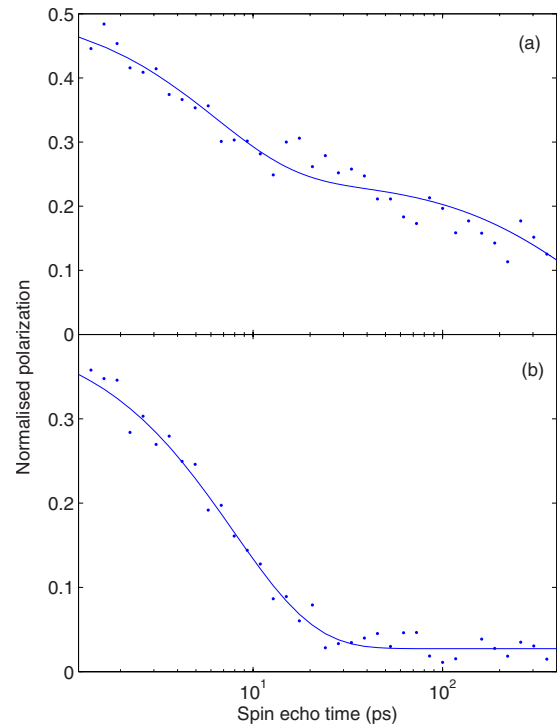
than at large times, resulting in a greater uncertainty in the fast component.) The fast behavior must correspond to a vertical component of motion, since it does not vanish for $\Delta\mathbf{K} \to 0$, and it dominates the measurements at low-momentum transfer. It appears similar to that of the anomalous line shapes reported by Alexandrowicz et al.[8] for coverages of Na/Cu(001) greater than $\theta = 0.065$ though, in the present work, we are able to separate the vertical and horizontal components to the motion.

Returning to the measurements at lower coverage, where the slow decay is well described by a single exponent, allows us to characterize the mechanism of diffusion through the momentum-transfer dependency of α, which we present in the left panel of Fig. 4. Measurements are shown for both the principal, high-symmetry azimuths of the Cu(001) surface at a coverage of 0.018 and a temperature of 155 K. Two significant features of the plot are: first, the prominent minimum seen in the inverse lifetimes at around 0.4 Å^{-1} along both azimuths and, second, the fact that the data along [100] (circles) lies above that for the [110] direction (squares), especially at large momentum transfer. The prominent minimum, known as a de Gennes[27] narrowing, can be ascribed to the effects of strong, repulsive, pairwise interactions between the adsorbates,[28] which generate a quasihexagonal overstructure with a characteristic separation. Differences in the data
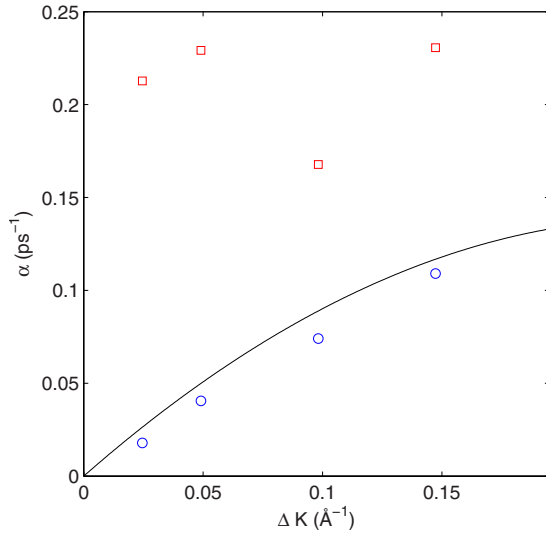
FIG. 3. (Color online) Dephasing rates obtained from polarization data at high coverage and low ΔK, $\theta = 0.084$, $\Delta K < 0.2$ Å^{-1}. Squares correspond to the fast component, which is evident in data between 1–10 ps. Circles correspond to the slower component, which is evident after approximately 7 ps. The solid line shows a smooth interpolation though 2D MD simulations using the calculated energy landscape described in Sec. IV. The close agreement between the calculations and the slow component confirms the identification of the slow component with lateral motion.

between the two principal azimuths indicates the degree of anisotropy in the potential-energy landscape.[29] Figure 4(b) gives the temperature dependence of the inverse lifetimes for a coverage of $\theta = 0.056$ at a momentum transfer of 0.5 Å^{-1}
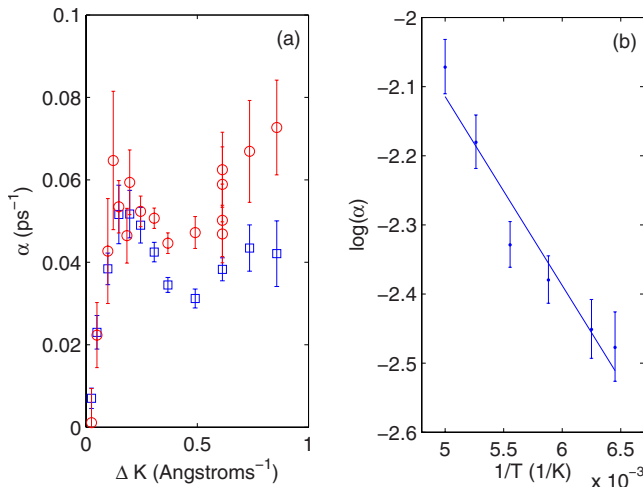

FIG. 4. (Color online) (a) Left-hand panel shows dephasing rates, α, as a function of momentum transfer for a coverage of $\theta = 0.018$ at 155 K. Open circles are measurements along the [100] azimuth while open squares are obtained along [110]. The prominent minimum near 0.4 Å^{-1} indicates strong adsorbate interactions and the difference between the two azimuths reflects the anisotropic energy landscape (see text). (b) Right-hand panel shows the temperature dependency of the dephasing rate over the range of 155–200 K for a coverage of $\theta = 0.056$ of potassium along the [100] azimuth at $\Delta K = 0.5$ Å^{-1}, presented as an Arrhenius plot. The slope of the line gives an activation energy for diffusion of 26 ± 2 meV.
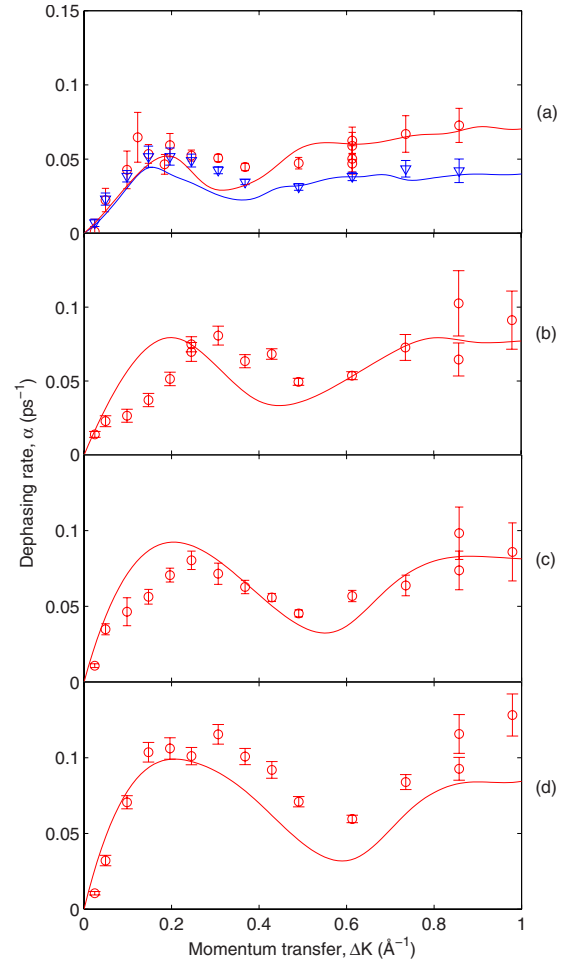

FIG. 5. (Color online) Dephasing rates from experiment, obtained from a single exponential fit in the long-time limit along the [100] (circles) and [110] azimuths [triangles in panel (a)] compared with 2D molecular-dynamics simulations (lines) (see Sec. V). The data is for a surface temperature of 155 K and coverages of: $\theta = $ (a) 0.018, (b) 0.032, (c) 0.045, and (d) 0.056.

along the [001], presented as an Arrhenius plot. A best fit line to the data gives an effective activation energy of 26 ± 2 meV. The effective activation energy may underestimate the true, adiabatic barrier;[30] nevertheless, the value obtained in the present work necessarily reflects a relatively small corrugation energy landscape, significantly lower than sodium[8] and slightly higher than that seen with caesium.[9]

In Fig. 5 we present the momentum-transfer dependency of α in the [100] direction for $\theta = 0.018$, 0.032, 0.045, and 0.056. The measurements, displayed as data points, show that the dephasing rate, α, increases with coverage. For example, the rate seen at the lowest coverage, $\theta = 0.018$, Fig. 5(a), is typically half that of the highest coverage, $\theta = 0.056$, Fig. 5(d). The values indicate a very high mobility of adsorbed potassium atoms similar in magnitude to that seen for the system of Cs/Cu(001).[9] In common with Cs, we see a momentum-transfer dependency that does not follow a simple sinusoidal single jump shape[22] but a shape that is rather flat. A flatter form for the ΔK variation is indicative of multiple jumps,[31,32] typically caused by a low adsorbate-

substrate friction. As the coverage increases, we also see the prominent de Gennes narrowing minimum at intermediate $\Delta\mathbf{K}$ move to higher momentum transfers, which is consistent with a reducing interadsorbate spacing in the overlayer structure.

In summary, the experimental data shows that the motion is predominantly hopping in an energy landscape with a corrugation lying between that observed in sodium and caesium. Motion is more frequent in the [100] direction indicating that the lowest barrier to motion occurs at the bridge site. At low coverage, the motion is entirely in the surface plane while, at higher and higher coverage, there is evidence of an increasing vertical component to the motion. We now discuss *ab initio* calculations of the energy landscape, which we use to analyze the experiment in more detail.

IV. DENSITY FUNCTIONAL THEORY

First principles simulations based on DFT have been used to estimate the PES for potassium adatoms, their dipole moment, and gain insight into the vertical motion observed in the experiments. In performing DFT calculations, a similar setup has been adopted as the one for a previous description of Na/Cu(001).[33] The Cu surface has been modeled by a slab composed of five layers in a periodically repeated supercell. The size of the supercell in the direction perpendicular to the surface amounted to 12 Cu(001) layers. Facing slabs are separated by a vacuum region of 11 Å [equivalent to six Cu(001) layers] with potassium atoms adsorbed on only one side of the slab. Dipole field corrections have been adopted to keep periodicity in the electrostatic potential without spurious electric fields inside the slab, as described by Bengtsson.[34] The two Cu layers opposite to the alkali atoms were kept fixed at the bulk truncated positions while the remaining atoms (including K) were relaxed together with the underlying metal layer to minimize the adiabatic total energy. All the results were obtained within a generalized gradient approximation for the exchange and correlation functional as proposed by Perdew, Burke, and Ernzerhof.[35] We used the plane-wave ultrasoft pseudopotential method,[36] as implemented in the PWSCF code of the QUANTUM-ESPRESSO distribution.[37] Pseudopotentials were derived from scalar-relativistic all-electron atomic calculations. Potassium and copper pseudopotentials have $3s$-$3p$-$4s$ and $3d$-$4s$ valence electrons, respectively. Nonlinear core corrections were used for Cu. Wave functions were expanded up to a kinetic-energy cutoff of 27 Ryd; the effective potential and the charge density up to 216 Ryd. The surface Brillouin-zone integration has been performed with the Monkhorst-Pack[38] scheme, adopting k-point meshes equivalent to a 12×12 mesh in the irreducible surface unit cell of Cu(001). The adsorption energy of potassium atoms was computed as

$$E^{\text{ads}} = E^{\text{tot}}_{\text{K/Cu(001)}} - E^{\text{tot}}_{\text{Cu(001)}} - E^{\text{tot}}_{\text{K}}, \qquad (1)$$

where the terms on the right-hand side are the total energy of the combined system, of the clean surface, and of the free neutral atom. The evaluation of E^{ads} with the adatom in different lateral positions and all other coordinates optimized
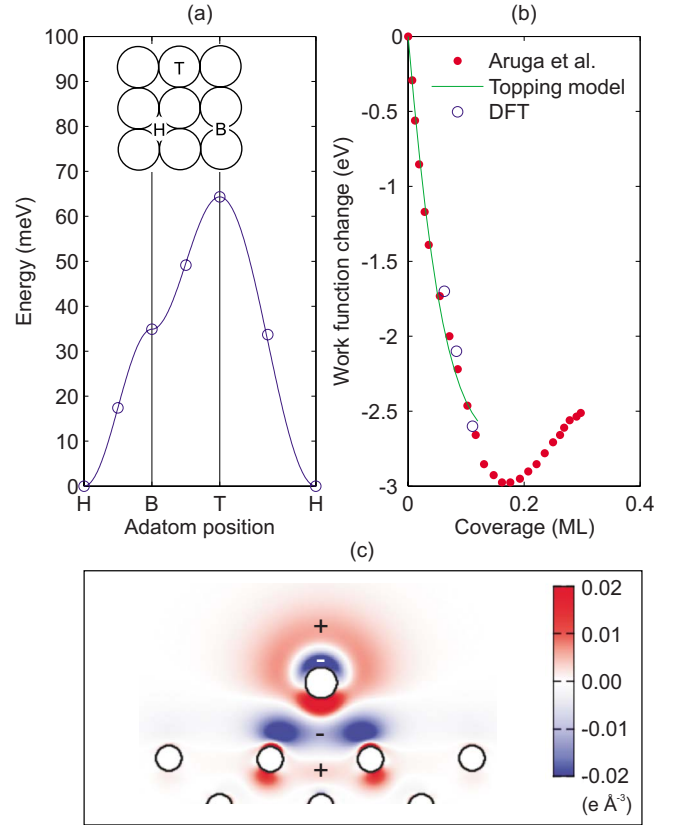

FIG. 6. (Color online) Potential-energy landscape derived from DFT calculations [panel (a)], fitted to simple cosine form (see text). Panel (b) shows the potassium coverage dependence of the work-function change from Aruga *et al.* (Ref. [13]) (filled circles) in comparison with values from DFT calculations in the current work (open circles). The line is a Topping model obtained from the experimental data at low coverage. Panel (c) illustrates the calculated charge rearrangement induced by adsorption of a potassium atom on the Cu(001) surface as compared to the sum of charge densities of the clean surface and the free neutral atom.

then yields a two-dimensional (2D) adiabatic PES for the potassium adatom, $V(x,y)$.

The PES was evaluated for the high-symmetry hollow, bridge, and top adsorption sites, plus three intermediate positions in between (corresponding to a 4×4 sampling of the surface unit cell) and a repeated 4×4 unit cell ($\theta=0.0625$) was used for this purpose. The result is shown in Fig. 6(a), taking the hollow site as a reference (it may be noted that the second and third terms on the right-hand side of Eq. (1) are common to all potassium positions and therefore do not contribute to the PES). We observe that a cosine expression interpolates the DFT values very well, in common with the other alkali atoms on Cu(001).[7] Accordingly, the following simple form of the PES,

$$V(x,y) = \frac{E_T}{4} + \frac{E_B}{2} + \frac{E_T}{4}\left[\cos\left(\frac{2\pi x}{a}\right) + \cos\left(\frac{2\pi y}{a}\right)\right]$$
$$+ \frac{1}{4}(E_T - 2E_B)\cos\left(\frac{2\pi x}{a}\right)\cos\left(\frac{2\pi y}{a}\right), \qquad (2)$$

will be used in the present work, as proposed in Ref. 39 and in recent studies of the dynamics of Na and Cs adatoms on Cu(001).[8,9] Here a is the Cu(001) surface lattice constant ($a=2.55$ Å); E_B and E_T are the energies in bridge and top sites, relative to the hollow one, evaluated as $E_B=35$ meV and $E_T=64$ meV.

The significant charge rearrangement induced by adsorption of the potassium atom at $\theta=0.0625$ is shown in Fig. 6(c) and results in a reduction in the surface work function by 1.70 eV. Estimating such reduction using DFT at the lower coverages investigated here would require much larger and computationally more expensive unit cells. Conversely, larger coverages are easily computed. We found a good agreement between our DFT results over a coverage range of $\theta=0.0625-0.111$, as evaluated in additional 4×3 and 3×3 simulation cells, and the work-function measurements of Aruga *et al.*,[13] as illustrated in Fig. 6(b).

Previous analysis of Na/Cu(001) has identified the origin of vertical motion due to electronic contributions altering the classical turning point for the He atom.[20] Additionally, it was shown that the changes are due to the dipole electric field associated with the adsorbates, which produce a different decay of the electron distribution on top of a Na atom as the local concentration of adsorbates fluctuates during diffusion. The arguments do not rely on specific properties of Na and will be now applied to the present potassium investigation.

In particular, a suitable definition of local concentration is given by the dipole-dipole interaction energy per adatom, E^{dd}.[20,21] In terms of that quantity, within a Wentzel-Kramers-Brillouin (WKB) approach one obtains a linear proportionality between the apparent height of the alkali adsorbate z^{CTP} and E^{dd}. The proportionality constant is estimated as

$$\frac{\partial z^{\mathrm{CTP}}}{\partial E^{\mathrm{dd}}} = \frac{2(z^{\mathrm{CTP}} - z_0)^2}{\mu k^2}, \qquad (3)$$

where z_0 is the adatom z coordinate, μ its dipole moment and k the decay rate of the WKB wave function in vacuum, as extracted by the DFT calculation of the electron density, where $\rho(z) \propto \exp(-2kz)$. For K/Cu(001) at $\theta=0.0625$, such dependence of the apparent height on the local concentration amounts to 2.5 Å/eV. This result is practically identical to the one in Na/Cu(001), because of compensations between the larger μ and the lower k when comparing K to Na, given $z^{\mathrm{CTP}} - z_0$ is relatively similar. Finally, we observe that the value of $\partial z^{\mathrm{CTP}}/\partial E^{\mathrm{dd}}$ will be reduced at lower coverages since, with a larger work function, k and μ both increase while z^{CTP} decreases (similar to the case of Na), and is consistent with the observed reduction of the vertical motion reported here.

V. MOLECULAR-DYNAMICS SIMULATIONS

To further our understanding of the underlying dynamics of the system, molecular dynamics and scattering simulations were carried out within a Langevin framework.[22,39] The Langevin MD approach has previously been used with considerable success in the interpretation of quasi-elastic helium atom scattering (QHAS) data on the dynamics of both sodium and caesium on Cu(001).[8,9] The simulations use an adiabatic adsorbate-substrate PES, in this case based on the DFT calculations described in the previous section. Energy transfer between adsorbate and substrate is modeled through a combination of frictional damping and random impulses which are scaled in magnitude with temperature using the same single frictional parameter according to fluctuation-dissipation theory.[40] The potassium-potassium interaction is modeled within the Lau and Kohn dipole repulsion potential.[41] The coverage-dependent dipole moment used by this model was deduced from the work-function measurements of Aruga *et al.*[13] and fitted with a Topping model.[42] At low coverage the Topping model reproduced the data well [as shown in Fig. 6(b)] with a polarizability of 45 Å^3 and a zero coverage dipole moment of 1.6 Åe (7.7 D).

Two-dimensional MD simulations involving 40 atoms were run for a total of 10 ns in 2 fs time steps. Simulated $I(\Delta\mathbf{K}, t_{se})$ curves were analyzed in the same manner as the experimental data with the resulting dephasing rates shown for comparison with experimental data in Fig. 5. A kinetic frictional dissipation of $\eta=1/(4.5\pm0.5)$ ps^{-1} was found to give best agreement with the data. Note that the friction coefficient is the only free parameter used to fit the simulations shown by the curves in Fig. 5.

The top panel of Fig. 5 compares the optimized MD simulations to the experimental data for the lowest coverage, $\theta=0.018$, along both principal azimuths, while the lower panels show increasing coverages in the [100] direction. Overall we see good agreement between the experimental and simulated values of α. In particular, for a coverage of $\theta=0.018$ we note that, at high-momentum transfer, the dephasing rates in both the [100] and [110] directions are reproduced well, implying that the DFT calculations have given an accurate estimate of the anisotropy of the PES. The most significant deviation of the simulation from the experiment is seen in the position and coverage dependence of the minimum at intermediate coverages. Since both the position and the coverage dependence arise from the strength and range of the adsorbate interactions, we can infer that the interactions are overestimated somewhat in the dipole-force model. The result is a minimum, that is, deeper in the simulations than in the experiment. The experimental data points at a coverage of $\theta=0.056$ lie consistently above the simulation (solid curve), which suggests some additional contribution in the experiment, that is, not present in the simulations. It is likely that, at this coverage, the experimental values of α are being influenced by the onset of vertical motion, in a similar manner to that seen in Fig. 3, an effect that is not modeled within the 2D MD simulations. Further temperature-dependent simulations (not shown) give an Arrhenius activation barrier to diffusion of 32 ± 6 meV, which is in agreement with the experimental value at the same conditions, further confirming the ability of the DFT calculations to produce an accurate model of the energy landscape.

The value of the adsorbate-substrate friction used to generate the curves in Fig. 5 may be compared with an estimate derived from the t-mode linewidth, as previously adopted for CO/Pt(111).[43] From previously published data,[17] we can place an upper limit of 0.7 meV on the linewidth of the potassium t mode; taking the line-shape model of Vega *et al.* [Eq. (2.33) in Ref. 44], and considering the first-order term,

results in a corresponding upper limit of 1.1 ps^{-1} to η, consistent with our value (1/4.5 ps^{-1}). Despite this agreement, we note that the friction predicted by the elastic continuum theory model (1/38 ps^{-1}) (Ref. 17) is much lower than our spin-echo result, as previously observed in the case of caesium.[9]

VI. SUMMARY AND CONCLUSIONS

Spin-echo measurements of the dynamics of low coverages of K/Cu(001) show hopping motion with repulsive adsorbate-adsorbate interactions from coverages as low as $\theta = 0.018$. Clear vertical motion similar to that previously observed for Na/Cu(001) is seen at $\theta = 0.084$. Langevin molecular-dynamics simulations using a PES deduced from DFT with bridge/top site energies of 35 and 64 meV, respectively, produce an optimal fit to the experimental data when combined with an adsorbate-substrate friction of 1/4.5 ps^{-1}. The DFT-based PES shows good agreement with both the anisotropy seen in the experimental data and the Arrhenius energy barrier. The relatively low potential barriers give rise to large numbers of long jumps in the data and place the system intermediate between sodium and caesium both in terms of the corrugation of the PES and the friction parameter. In contrast with Na/Cu(001) but in common with Cs/Cu(001), the dipole-dipole model appears to be of limited accuracy in modeling the K/Cu(001) data.

*hh242@cam.ac.uk

†Also at Department of Chemistry, Technion–Israel Institute of Technology, Haifa 32000, Israel.

1 I. Langmuir, Phys. Rev. **22**, 357 (1923).

2 R. D. Diehl and R. McGrath, Surf. Sci. Rep. **23**, 43 (1996).

3 N. D. Lang, Phys. Rev. B **4**, 4234 (1971).

4 H. Ishida, Phys. Rev. B **42**, 10899 (1990).

5 G. Pacchioni and P. S. Bagus, Surf. Sci. **269-270**, 669 (1992).

6 J. Bormet, J. Neugebauer, and M. Scheffler, Phys. Rev. B **49**, 17242 (1994).

7 G. Fratesi, Phys. Rev. B **80**, 045422 (2009).

8 G. Alexandrowicz, A. P. Jardine, H. Hedgeland, W. Allison, and J. Ellis, Phys. Rev. Lett. **97**, 156103 (2006).

9 A. P. Jardine, G. Alexandrowicz, H. Hedgeland, R. D. Diehl, W. Allison, and J. Ellis, J. Phys.: Condens. Matter **19**, 305010 (2007).

10 T. Aruga, H. Tochihara, and Y. Murata, Phys. Rev. Lett. **52**, 1794 (1984).

11 T. Aruga, H. Tochihara, and Y. Murata, Surf. Sci. **158**, 490 (1985).

12 T. Aruga, H. Tochihara, and Y. Murata, Surf. Sci. Lett. **175**, L725 (1986).

13 T. Aruga, H. Tochihara, and Y. Murata, Phys. Rev. B **34**, 8237 (1986).

14 H. L. Meyerheim, I. K. Robinson, V. Jahns, P. J. Eng, and W. Moritz, Z. Kristallogr. **208**, 73 (1993).

15 H. L. Meyerheim, J. Wever, V. Jahns, W. Moritz, P. J. Eng, and I. K. Robinson, Physica B **198**, 66 (1994).

16 M.-S. Chen, S. Mizuno, and H. Tochihara, Surf. Sci. **601**, 5162 (2007).

17 P. Senet, J. P. Toennies, and G. Witte, Chem. Phys. Lett. **299**, 389 (1999).

18 A. Reichmuth, A. P. Graham, H. G. Bullman, W. Allison, and G. E. Rhead, Surf. Sci. **307-309**, 34 (1994).

19 B. N. J. Persson and R. Ryberg, Phys. Rev. B **32**, 3586 (1985).

20 G. Fratesi, G. Alexandrowicz, M. I. Trioni, G. P. Brivio, and W. Allison, Phys. Rev. B **77**, 235444 (2008).

21 M. I. Trioni, G. Fratesi, S. Achilli, and G. P. Brivio, J. Phys.: Condens. Matter **21**, 264003 (2009).

22 A. P. Jardine, J. Ellis, and W. Allison, J. Phys.: Condens. Matter **14**, 6173 (2002).

23 G. Alexandrowicz and A. P. Jardine, J. Phys.: Condens. Matter **19**, 305001 (2007).

24 F. Mezei, *Neutron Spin Echo*, Springer Lecture Notes in Physics (Springer, Berlin, 1980).

25 L. van Hove, Phys. Rev. **95**, 249 (1954).

26 P. Fouquet, A. P. Jardine, S. Dworski, G. Alexandrowicz, W. Allison, and J. Ellis, Rev. Sci. Instrum. **76**, 053109 (2005).

27 P. G. deGennes, Physica (Amsterdam) **25**, 825 (1959).

28 A. P. Jardine, G. Alexandrowicz, H. Hedgeland, W. Allison, and J. Ellis, Phys. Chem. Chem. Phys. **11**, 3355 (2009).

29 G. Alexandrowicz, A. P. Jardine, P. Fouquet, S. Dworski, W. Allison, and J. Ellis, Phys. Rev. Lett. **93**, 156103 (2004).

30 A. P. Jardine, J. Ellis, and W. Allison, J. Chem. Phys. **120**, 8724 (2004).

31 C. T. Chudley and R. J. Elliot, Proc. Phys. Soc. London **77**, 353 (1961).

32 L. Y. Chen, M. R. Baldan, and S. C. Ying, Phys. Rev. B **54**, 8856 (1996).

33 G. P. Brivio, G. Butti, S. Caravati, G. Fratesi, and M. I. Trioni, J. Phys.: Condens. Matter **19**, 305005 (2007).

34 L. Bengtsson, Phys. Rev. B **59**, 12301 (1999).

35 J. P. Perdew, K. Burke, and M. Ernzerhof, Phys. Rev. Lett. **77**, 3865 (1996).

36 D. Vanderbilt, Phys. Rev. B **41**, 7892 (1990).

37 P. Giannozzi, S. Baroni, N. Bonini, M. Calandra, R. Car, C. Cavazzoni, D. Ceresoli, G. L. Chiarotti, M. Cococcioni, I. Dabo, A. Dal Corso, S. de Gironcoli, S. Fabris, G. Fratesi, R. Gebauer, U. Gerstmann, C. Gougoussis, A. Kokalj, M. Lazzeri, L. Martin-Samos, N. Marzari, F. Mauri, R. Mazzarello, S. Paolini, A. Pasquarello, L. Paulatto, C. Sbraccia, S. Scandolo, G. Sclauzero, A. P. Seitsonen, A. Smogunov, P. Umari, and R. M. Wentzcovitch, J. Phys.: Condens. Matter **21**, 395502 (2009).

38 H. J. Monkhorst and J. D. Pack, Phys. Rev. B **13**, 5188 (1976).

39 J. Ellis, A. P. Graham, F. Hofmann, and J. P. Toennies, Phys. Rev. B **63**, 195408 (2001).

40 R. Kubo, Rep. Prog. Phys. **29**, 255 (1966).

41 W. Kohn and K. H. Lau, Solid State Commun. **18**, 553 (1976).

42 J. Topping, Proc. R. Soc. London, Ser. A **114**, 67 (1927).

43 A. P. Graham and J. P. Toennies, Europhys. Lett. **42**, 449 (1998).

44 J. L. Vega, R. Guantes, S. Miret-Artes, and D. A. Micha, J. Chem. Phys. **121**, 8580 (2004).